

# DISCONTINUOUS GALERKIN METHODS APPLIED TO TWO-PHASE FLOW PROBLEMS

OWEN J. ESLINGER<sup>†1</sup> AND MARY F. WHEELER<sup>2</sup>

<sup>†</sup> Corresponding Author

<sup>1</sup>Information Technology Laboratory, U.S. Army Engineer Research and Development Center, 3909 Halls Ferry Road, Vicksburg, MS, 39180, USA,  
Owen.J.Eslinger@erd.c.usace.army.mil

<sup>2</sup>Center for Subsurface Modeling (CSM-ICES), 201 E. 24th Street, The University of Texas at Austin, Austin, TX 78712, USA

## ABSTRACT

A family of discontinuous Galerkin (DG) finite element methods are proposed to solve two-phase flow equations, such as the air-water system that arises in shallow subsurface flow problems. Two time-splitting approaches are described that incorporate either primal formulations, such as the Oden-Baumann-Babuska DG (OBB-DG), Symmetric Interior Penalty Galerkin (SIPG), Non-Symmetric Interior Penalty Galerkin (NIPG), and Incomplete Interior Penalty Galerkin (IIPG), or the local discontinuous Galerkin (LDG) method applied to the saturation equation. The two-phase flow equations presented are discretized with an implicit pressure/explicit saturation (IMPES) formulation.

The IMPES formulation introduced in this work uses a primal DG formulation to solve the pressure equation implicitly at every time-step, followed by an explicit LDG scheme for the saturation equation. The LDG scheme advances in time via explicit Runge-Kutta time-stepping while employing a Kirchoff transformation for the local solution of the degenerate diffusion term.

DG finite element methods are naturally suited to problems of subsurface flow and transport. They can handle general meshes that may be nonconforming, treat higher order approximations, and are locally mass conservative, among many other desirable properties. In particular, due to different rock properties at the interface between two materials, fluid saturations may be discontinuous. Therefore DG methods are a natural approach for this class of problems. Computational results demonstrating that the proposed IMPES method will hold capillary barriers while using two capillary pressure curves in different materials are presented.

## 1. INTRODUCTION

The popularity of discontinuous Galerkin (DG) and local discontinuous Galerkin (LDG) finite element methods has been growing over the past decade in a variety of computational arenas due to increases in available computational power and the many attractive features of DG methods. These features include but are not limited to the ability to

handle general meshes that may be nonconforming; the use of general element types such as tetrahedra, prisms, and bricks in three dimensions; the ability to treat higher order approximations, with easy handling of  $h$ - $p$  adaptivity; the local mass conservation property; less numerical diffusion than continuous methods for the modeling of reactive transport; the ability to handle full diffusion tensors; and the ability to handle discontinuous coefficients throughout the domain. Thus DG offers a natural approach to the handling of discontinuous saturations that occur due to changes in rock properties, as well as a host of other geologic features, such as faults and fissures.

In this work, we propose a DG-LDG method for two-phase immiscible flow problems in porous media. In §2, we will present the notation used throughout this work. In §3 we will state one of the many pressure-saturation formulations of the two-phase flow equations, which we will discretize with an implicit pressure explicit saturation (IMPES) primal DG-LDG discretization, taking advantage of Kirchoff transformations in the LDG saturation step. In §4, we will present numerical results from a two-phase flow simulation in which we demonstrate that our method can handle capillary barriers between two different material types. Finally, in §5, we will summarize the main results of this work and suggest directions for further research.

## 2. NOTATION

We must first detail some of the notation used throughout this work. Let  $\Omega \subset \mathbb{R}^3$  be a domain with the external boundary denoted as  $\Gamma = \partial\Omega$ . Let  $\mathcal{E}_h = \{E_i\}_{N_h} \subset \mathbb{R}^3$  be a partition of the domain with  $N_h$  elements. We assume that this discretization is non-degenerate, quasi-uniform, and composed of tetrahedra, bricks, or prisms in 3D. We allow that it is possibly nonconforming. The boundary of some generic element  $E$  will be denoted  $\partial E$ . The internal faces, faces shared by two elements, will be written as  $e_{lk}$ , where  $e_{lk}$  denotes the face shared by elements  $E_l$  and  $E_k$ . We will also generally denote the unit normal to the face  $e_{lk}$  as “out of” element  $E_l$  and “in to”  $E_k$ . Let  $\Gamma_h$  denote the set of all internal faces of the discretization.

For an integer  $r$  we associate a finite element subspace of discontinuous piecewise polynomials:  $\mathcal{D}_r(\mathcal{E}_h) = \{v : v|_E \in P_r(E) \ \forall E \in \mathcal{E}_h\}$ , where  $P_r(E)$  is a discrete space containing the set of polynomials of total degree less than or equal to  $r$  on  $E$ . We could also use the set of tensor product polynomials,  $Q_r(E)$  that have individual degree less than or equal to  $r$ .

Along the face  $e_{lk}$ , the *average* of  $\psi \in \mathcal{D}_r(\mathcal{E}_h)$  is denoted by the curly bracket notation, on the left,

$$\{\psi\}_{lk} \equiv \frac{\psi|_l + \psi|_k}{2} \quad [\psi]_{lk} \equiv \psi|_l - \psi|_k$$

where  $\psi|_l$  is the trace of  $\psi$  for element  $E_l$ . The *jump* in  $\psi$  across the face  $e_{lk}$  is written with the square bracket notation, on the right. For both the average and jump terms, if we are on a face along the boundary of the domain,  $e_j \in \partial E_j \cap \Gamma \neq \emptyset$ , then we define  $\{\psi\}_j = \psi|_j = [\psi]_j$  allowing for a degree of continuity in our notation.

Let  $\psi, \varphi \in \mathcal{D}_r(\mathcal{E}_h)$ . We define the zero-order penalty term along all of the interior faces (in 3D) of the discretization

$$J_{0,\Gamma_h}^{\sigma,r}(\varphi, \psi) = \sum_{e \in \Gamma_h} \frac{r\sigma_e}{|e|^\beta} \int_e [\varphi][\psi] ds,$$

where  $r$  is the polynomial order of approximation, and  $\sigma_e$  is a discrete positive function that takes on a constant value on each face. We have  $0 \leq \sigma_0 \leq \sigma_e \leq \sigma_m$  for  $\forall e \in \Gamma_h$ . We let  $|e|$  denote the measure of  $e$  and set  $\beta = 1/2$  for 3D problems.

For the pressure-saturation formulation, we will use the following symbols. We will assume that there are two immiscible phases: a wetting and a nonwetting phase, denoted with the subscripts  $w$  and  $n$ , respectively. Therefore, the phase pressures for each of the two phases will be written as  $P_w$  and  $P_n$  with capillary pressure  $P_c = P_n - P_w$ . Likewise, the saturations of each phase will be denoted by  $S_w, S_n$ , densities as  $\rho_w, \rho_n$ , and viscosities as  $\mu_w, \mu_n$ . For the porous medium,  $\phi$  will denote porosity, the tensor  $\mathbf{K}$  the intrinsic permeability, and  $\kappa_w$  the relative permeability of the wetting phase, etc. We will write the mobility  $\lambda_w = \kappa_w/\mu_w$  and the variant  $\hat{\lambda}_w = \rho_w\lambda_w$ . We will take advantage of standard empirical results that allow us to write the capillary pressure and relative permeabilities as functions of the wetting phase saturation, e.g.,  $P_c = P_c(S_w)$  and  $\kappa_w = \kappa_w(S_w)$ . We will also use the well known Darcy velocity

$$\mathbf{u}_w = -\frac{\kappa_w}{\mu_w} \mathbf{K}(\nabla P_w - \rho_w g \nabla D_z), \quad (1)$$

where  $g \nabla D_z$  represents a gravity vector pointing “down.” For simplicity, we also work with the following notation, defining total mobility  $\lambda_t$  and total velocity  $\mathbf{u}_t$  as follows:

$$\begin{aligned} \lambda_t &= \lambda_n + \lambda_w & \hat{\lambda}_t &= \hat{\lambda}_n + \hat{\lambda}_w \\ \mathbf{u}_t &= \mathbf{u}_n + \mathbf{u}_w & \hat{\mathbf{u}}_t &= \rho_n \mathbf{u}_n + \rho_w \mathbf{u}_w. \end{aligned}$$

Extending the “hat” notation to these definitions allows us to write a mass flux  $\hat{\mathbf{u}}_t$  in addition to the volumetric flux  $\mathbf{u}_t$ . Variables with a superscript, e.g.,  $\lambda_t^n$ , indicate that the variable uses data from the  $n^{\text{th}}$  time-step.

### 3. DG DISCRETIZATION OF THE TWO-PHASE FLOW EQUATIONS

We begin by stating, without derivation, a pressure-saturation formulation of the two-phase flow equations. These equations may be derived from the conservation of mass equation and Darcy’s Law for each of the two phases, the capillary pressure relationship and the two-phase saturation relationship ( $S_w + S_n = 1$ ). The four unknowns will be the two phase pressures  $P_w$  and  $P_n$  and the two phase saturations  $S_w$  and  $S_n$ . We will choose the wetting phase pressure and saturation ( $P_w, S_w$ ) as the primary unknowns. For more details and a complete derivation see [Eslinger, 2005]. For a general introduction to multiphase flow problems and a complete treatment of the terminology, see [Helmig, 1997], [Bear, 1972], and the many references therein.

**3.1. Two-Phase Flow Formulation.** The following equation will be referred to as the *Pressure Equation*:

$$\begin{aligned} \frac{\partial(\phi\rho_w S_w + \phi\rho_n S_n)}{\partial t} - \nabla \cdot (\hat{\lambda}_t \mathbf{K} \nabla P_w) &= \rho_w \hat{q}_w + \rho_n \hat{q}_n \\ - \nabla \cdot \left( -\hat{\lambda}_n \left( \frac{\partial P_c(S_w)}{\partial S_w} \right) \mathbf{K} \nabla S_w + (\hat{\lambda}_w \rho_w + \hat{\lambda}_n \rho_n) \mathbf{K} g \nabla D_z \right). \end{aligned} \quad (2a)$$

Here  $\hat{q}_w$  and  $\hat{q}_n$  are volumetric source and sink terms. The boundary of domain  $\partial\Omega = \Gamma$  will be split into a Dirichlet component  $\Gamma_D$  and a Neumann component  $\Gamma_N$  such that  $\Gamma_D \cap \Gamma_N = \emptyset$  and  $\Gamma = \Gamma_D \cup \Gamma_N$ . Thus, our boundary conditions will be written as

$$P_w = P_{dir} \quad \text{on} \quad \Gamma_D \quad \text{and} \quad \hat{\mathbf{u}}_t \cdot \boldsymbol{\nu} = \gamma_N \quad \text{on} \quad \Gamma_N. \quad (2b)$$

We also provide the *Saturation Equation* as:

$$\begin{aligned} \frac{\partial(\phi\rho_w S_w)}{\partial t} + \nabla \cdot \left( \frac{\rho_w \lambda_n \lambda_w}{\lambda_t} \mathbf{K} \nabla P_c \right) &= \rho_w \hat{q}_w - \nabla \cdot \left( \frac{\rho_w \lambda_w}{\lambda_t} \mathbf{u}_t \right) \\ - \nabla \cdot \left( \frac{\rho_w \lambda_w \lambda_n}{\lambda_t} (\rho_w - \rho_n) \mathbf{K} g \nabla D_z \right). \end{aligned} \quad (3a)$$

The boundary conditions for this equation are divided into inflow and outflow portions of the domain boundary,  $\partial\Omega = \Gamma = \Gamma_{in} \cup \Gamma_{out}$ . The inflow portion is defined as  $\Gamma_{in} = \{\mathbf{x} \in \partial\Omega : \mathbf{u}_t \cdot \boldsymbol{\nu} < 0\}$ , and the outflow portion is defined as  $\Gamma_{out} = \{\mathbf{x} \in \partial\Omega : \mathbf{u}_t \cdot \boldsymbol{\nu} \geq 0\}$ , where  $\boldsymbol{\nu}$  is the unit outward normal along the domain boundary. In either case, we assume that fluids do not diffuse across the boundary due to capillary pressure differences,  $(\mathbf{K} \nabla P_c) \cdot \boldsymbol{\nu} = 0$ . Thus we have

$$-\left( \frac{\rho_w \lambda_n \lambda_w}{\lambda_t} \mathbf{K} \nabla P_c \right) \cdot \boldsymbol{\nu} = 0 \quad \text{on} \quad \Gamma_{out} \quad (3b)$$

$$\left( S_w \mathbf{u}_t - \frac{\rho_w \lambda_n \lambda_w}{\lambda_t} \mathbf{K} \nabla P_c \right) \cdot \boldsymbol{\nu} = S_{in} \mathbf{u}_t \cdot \boldsymbol{\nu} \quad \text{on} \quad \Gamma_{in}. \quad (3c)$$

**3.2. Pressure Equation: Implicit Primal DG Discretization.** We solve the above Pressure-Saturation formulation with an IMPES approach. Given  $(P_w^n, S_w^n)$  from the previous time-step, we will update each of these primary variables sequentially. Therefore, we can write the Pressure Equation using an implicit primal DG formulation. Here we will take  $\psi \in \mathcal{D}_r(\mathcal{E}_h)$  as an approximation of the new wetting phase saturation,  $P_w^{n+1}$ , and  $\varphi \in \mathcal{D}_r(\mathcal{E}_h)$  as a test function. On the left-hand side we have

$$\begin{aligned} \sum_{N_h} \int C_1 \psi \varphi \, dE &+ \sum_{N_h} \int (\nabla \varphi) \cdot (\hat{\lambda}_t^n \mathbf{K} \nabla \psi) \, dE + J_{0, \Gamma_h}^{\sigma, r}(\varphi, \psi) \\ &- \sum_{e \in \Gamma_h \cup \Gamma_D} \int_e [\varphi] \{ (\hat{\lambda}_t^n \mathbf{K} \nabla \psi) \cdot \boldsymbol{\nu}_e \} \, ds + J_{0, \Gamma_D}^{\sigma, r}(\varphi, \psi) \\ &+ s_{form} \sum_{e \in \Gamma_h \cup \Gamma_D} \int_e [\psi] \{ (\hat{\lambda}_t^n \mathbf{K} \nabla \varphi) \cdot \boldsymbol{\nu}_e \} \, ds. \end{aligned}$$

The various primal DG forms differ in their handling of the penalty term and their values for  $s_{form}$ . We will take  $s_{form} = +1$  for OBB-DG and NIPG,  $s_{form} = 0$  for IIPG, and

$s_{form} = -1$  for SIPG. For further details, see [Dawson et al., 2004] and references therein. On the right-hand side we have

$$\begin{aligned}
& \sum_{N_h} \int \left( -C_2 + \rho_w^n \hat{q}_w^{n+1} + \rho_n^n \hat{q}_n^{n+1} \right) \varphi \, dE + \sum_{e \in \Gamma_N} \int_e \varphi \gamma_N \, ds + J_{0, \Gamma_D}^{\sigma, r}(\varphi, P_{dir}) \\
& + \sum_{N_h} \int \left( -\hat{\lambda}_n^n \left( \frac{\partial P_c(S_w^n)}{\partial S_w} \right) \mathbf{K} \nabla S_w^n \right) \cdot (\nabla \varphi) \, dE \\
& + \sum_{N_h} \int \left( (\hat{\lambda}_w^n \rho_w^n + \hat{\lambda}_n^n \rho_n^n) \mathbf{K} g \nabla D_z \right) \cdot (\nabla \varphi) \, dE \\
& - \sum_{e \in \Gamma_h \cup \Gamma_D} \int_e [\varphi] \left\{ \left( -\hat{\lambda}_n^n \left( \frac{\partial P_c(S_w^n)}{\partial S_w} \right) \mathbf{K} \nabla S_w^n \right) \cdot \nu_e \right\} \, ds \\
& - \sum_{e \in \Gamma_h \cup \Gamma_D} \int_e [\varphi] \left\{ \left( (\hat{\lambda}_w^n \rho_w^n + \hat{\lambda}_n^n \rho_n^n) \mathbf{K} g \nabla D_z \right) \cdot \nu_e \right\} \, ds \\
& + s_{form} \sum_{e \in \Gamma_D} \int_e [P_{dir}] \left\{ (\hat{\lambda}_t^n \mathbf{K} \nabla \varphi) \cdot \nu_e \right\} \, ds.
\end{aligned}$$

The values of  $C_1$  and  $C_2$  above come from the first-order discretization of the time derivative in Equation (2a), see [Eslinger, 2005].

**3.3. Saturation Equation: Explicit LDG Discretization.** We will now use an explicit LDG discretization of Equation (3a) to obtain the saturation at the new time-step,  $S_w^{n+1}$ . At the beginning of the computation  $(P_w^{n+1}, S_w^n)$  will be our most recent approximations to the primary variables. Explicit methods like this one are very straightforward in the computational sense. Some of the costs associated with DG methods are mitigated by the purely local computations needed for the diffusion term. Smaller time-steps are required, but this can be offset by taking a large, implicit pressure step, followed by many, faster explicit saturation steps.

We introduce the *Kirchoff transform* to be used on the diffusion term, defining the variable  $D$  as a function of  $S_w$ ,

$$D(S_w) = - \int_0^{S_w} \frac{\rho_w \lambda_w(\xi) \lambda_n(\xi)}{\lambda_t(\xi)} \left( \frac{\partial P_c}{\partial \xi}(\xi) \right) \partial \xi.$$

Notice that this equation is a monotonically increasing function of water saturation, and it can be calculated well in advance of any simulations. Note, as well, that

$$\nabla D(S_w) = - \frac{\rho_w \lambda_w(S_w) \lambda_n(S_w)}{\lambda_t(S_w)} \left( \frac{\partial P_c(S_w)}{\partial S_w} \right) \nabla S_w.$$

Since  $\nabla P_c = (\partial P_c / \partial S_w) \nabla S_w$ , we can see that

$$\mathbf{K} \nabla D(S_w) = - \left( \frac{\rho_w \lambda_n \lambda_w}{\lambda_t} \mathbf{K} \nabla P_c \right).$$

Compare this to the diffusion term in Equation (3a).

With the approximation to the water saturation from the previous time-step  $S_w^n$ , we will outline an LDG method to obtain an approximation to the time derivative  $(\partial S_w / \partial t)^n$ .

This approximation, in conjunction with Runge-Kutta time-stepping, will allow us to obtain our new approximation for water saturation,  $S_w^{n+1}$ .

We first solve a local problem to find our approximation  $\bar{\mathbf{Y}}^n$ , where  $\bar{\mathbf{Y}}^n = \nabla D(S_w^n)$ ,

$$\begin{aligned} \int_E \bar{\mathbf{Y}}^n \cdot \bar{\boldsymbol{\Psi}} \, dE &= - \int_E D(S_w^n) (\nabla \cdot \bar{\boldsymbol{\Psi}}) \, dE + \int_{\partial E \cap \Gamma_{in}} \{D(S_{in})\} [\bar{\boldsymbol{\Psi}} \cdot \boldsymbol{\nu}] \, ds \\ &+ \int_{\partial E \setminus \Gamma_{in}} \{D(S_w^n)\} [\bar{\boldsymbol{\Psi}} \cdot \boldsymbol{\nu}] \, ds. \end{aligned}$$

The capillary pressure curve used for  $D(S_w^n)$  is allowed to be unique for each material. The last term above, which involves element boundaries, easily handles different capillary pressure curves in different materials. Another local problem gives  $\bar{\mathbf{Z}}^n = -\mathbf{K}\bar{\mathbf{Y}}^n$ ,

$$\int_E \bar{\mathbf{Z}}^n \cdot \bar{\boldsymbol{\Phi}} \, dE = \int_E (-\mathbf{K}\bar{\mathbf{Y}}^n) \cdot \bar{\boldsymbol{\Phi}} \, dE.$$

We now solve a global problem for  $\psi \approx (\partial S_w / \partial t)^n$ . The left-hand side will be

$$\sum_{N_h} \int \phi \rho_w^{n+1} \psi \varphi \, dE.$$

On the right-hand side of this equation we will have

$$\begin{aligned} &\sum_{N_h} \int \rho_w^{n+1} \hat{q}_w^{n+1} \varphi \, dE + \sum_{N_h} \int \left( \frac{\rho_w^{n+1} \lambda_w^n}{\lambda_t^n} \hat{\mathbf{u}}_t^n \right) \cdot (\nabla \varphi) \, dE + \sum_{N_h} \int (\bar{\mathbf{Z}}^n) \cdot (\nabla \varphi) \, dE \\ &- \sum_{e \in \Gamma_{in}} \int_e \frac{\rho_w^{n+1} \lambda_w(S_{in})}{\lambda_t(S_{in})} \{ \hat{\mathbf{u}}_t^n \cdot \boldsymbol{\nu} \} [\varphi] \, ds - \sum_{e \in \Gamma_h \cup \Gamma_{in}} \int_e \{ \bar{\mathbf{Z}}^n \cdot \boldsymbol{\nu} \} [\varphi] \, ds \\ &- \sum_{e \in \Gamma_h \cup \Gamma_{out}} \int_e \left( \frac{\rho_w^{n+1} \lambda_w^n}{\lambda_t^n} \right)^* \{ \hat{\mathbf{u}}_t^n \cdot \boldsymbol{\nu} \} [\varphi] \, ds \\ &+ \sum_{N_h} \int \left( \frac{\rho_w^{n+1} \lambda_w^n \lambda_n^n}{\lambda_t^n} (\rho_w^{n+1} - \rho_n^{n+1}) \mathbf{K} g \nabla D_z \right) \cdot (\nabla \varphi) \, dE \\ &- \sum_{e \in \Gamma_h \cup \Gamma_{out}} \int_e \left\{ \left( \frac{\rho_w^{n+1} \lambda_w^n \lambda_n^n}{\lambda_t^n} (\rho_w^{n+1} - \rho_n^{n+1}) \mathbf{K} g \nabla D_z \right) \cdot \boldsymbol{\nu} \right\} [\varphi] \, ds \\ &- \sum_{e \in \Gamma_{in}} \int_e \left\{ \left( \frac{\rho_w^{n+1} \lambda_w(S_{in}) \lambda_n(S_{in})}{\lambda_t(S_{in})} (\rho_w^{n+1} - \rho_n^{n+1}) \mathbf{K} g \nabla D_z \right) \cdot \boldsymbol{\nu} \right\} [\varphi] \, ds. \end{aligned}$$

Here,  $\varphi \in \mathcal{D}_r(\mathcal{E}_h)$  is the test function.

#### 4. NUMERICAL RESULTS

The proposed finite element discretization has been validated using empirical results from laboratory settings, see [Eslinger, 2005]. Specifically, we examined the 1D problem of ponded infiltration into a bounded column from [Touma and Vauclin, 1986] and the 2D problem of constant flux into the unsaturated zone from [Vauclin et al., 1979]. The primal DG-LDG formulation captured the wetting phase front exactly in each case.

FIGURE 1. 2D Entry Pressure Problem: There are two materials in the oil/water system. Shown on the left is the domain. In red is the higher permeable material, Material 1, and in blue, Material 2. Shown on the right are the capillary pressure curves for both materials.

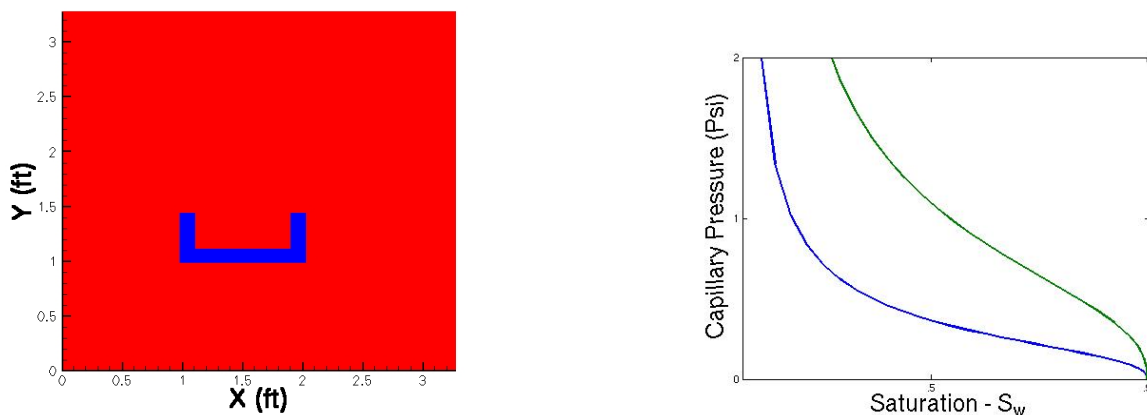
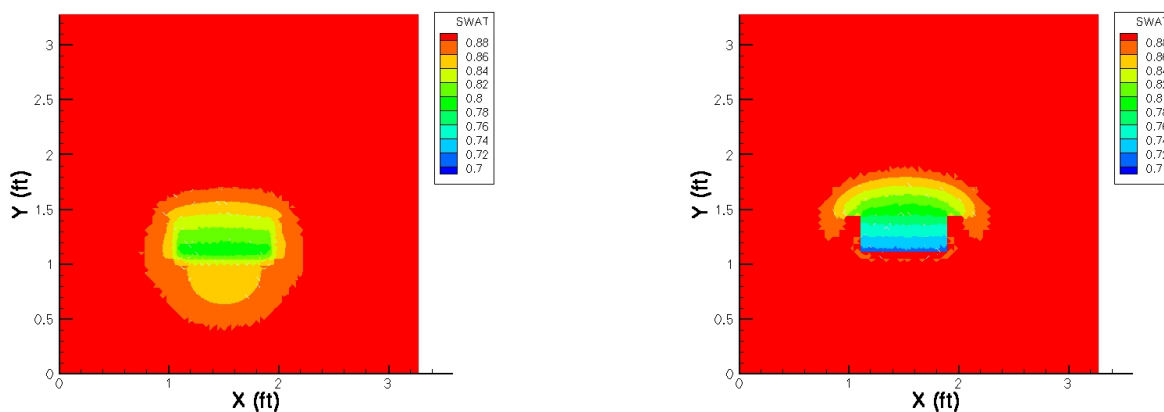


FIGURE 2. 2D Simulations at 24 hours of simulated time: On the left, we have used one capillary pressure curve for both materials. On the right, we have used different capillary pressure curves for the different materials.



In this section we will demonstrate another particularly attractive attribute of DG methods for two-phase flow problems, namely, their ability to handle different relative permeability and capillary pressure curves in different materials. Here, we will use two slightly compressible fluids. The wetting phase will be water and the nonwetting phase will be a heavy oil with  $\rho_n = (1.1)\rho_w$  and viscosity  $\mu_n = 13 \text{ cp}$ .

The capillary pressure curves used in these numerical simulations are shown on the right in Figure 1. Note that the capillary pressure values on the higher curve are exactly 3 times the values of the lower curve. As intrinsic permeability and capillary pressure are related, the difference in permeability should be a factor of approximately  $3^2 = 9$ . In the

cases shown, the permeability of the material corresponding to the higher curve will be  $\mathbf{K}_2 = 1$  Darcy and the lower curve will correspond to  $\mathbf{K}_1 = 10$  Darcy.

The domain is a  $1\text{ m} \times 1\text{ m}$  box in 2D with two materials present. The exact layout of materials can be seen on the left in Figure 1, where red represents the more permeable Material 1, and blue represents the less permeable Material 2. Initially, dense oil will be deposited inside, along the bottom of this formation, i.e., inside the “U.” Ideally, due to the small amount of oil present, the capillary barrier will be maintained, and oil will not enter Material 2. This is exactly what occurs, as seen on the right in Figure 2. There is some diffusion acting against gravity, but the dense oil is pooling at the interface between the materials, and the capillary barrier “holds.” For comparison, a second simulation was performed, in which one capillary pressure curve, the original curve of Material 1, was used for both materials. As we can see on the left in Figure 2, oil has not only entered Material 2, but has diffused through it and reentered Material 1. Indeed we see a plume of oil in Material 1 at the bottom of the domain. These are quite different results. Obviously, the use of two capillary pressure curves is physically correct, and it is captured by our primal DG-LDG method.

The computational mesh used in all figures contains 10,000 triangular elements approximately  $1\text{ cm}^2$ . Time-steps of 15 sec were taken for the pressure equation, and two saturation steps were taken for every pressure step. For the pressure step we used IIPG and  $r = 2$ , quadratic approximations. For the saturation step, we used  $r = 1$ , linear approximations. First-order Runge-Kutta time-stepping was also used.

## 5. CONCLUSION

The DG-LDG method described is a promising technique for immiscible two-phase flow simulations. Specifically, it was shown that this method can handle discontinuous jumps in material types, and, in addition, can easily deal with different capillary pressure curves for these different materials. There may be concerns with the additional work required for primal DG methods. However, it must be noted that it is not necessary for the pressure field to be solved using DG methods. It is quite possible that the pressure equation could be solved with another methodology, e.g., mixed finite elements, while retaining the LDG explicit saturation solve.

## REFERENCES

- Bear, 1972. Bear, J. (1972), *Dynamics of Fluids in Porous Media*, Elsevier Publishing Company, Inc., New York, NY, USA.
- Dawson et al., 2004. Dawson, C., Sun, S., and Wheeler, M. F. (2004), Compatible algorithms for coupled flow and transport. *Computer Methods in Applied Mechanics and Engineering* 193, 2565-2580.
- Eslinger, 2005. Eslinger, O. J. (2005), Discontinuous Galerkin Finite Element Methods Applied to Two-Phase, Air-Water Flow Problems, Ph.D. Dissertation, The Univ. of Texas at Austin, Austin, TX, USA.
- Helmig, 1997. Helmig, R. (1997), *Multiphase Flow and Transport Processes in the Subsurface: A Contribution to the Modeling of Hydrosystems*, Springer-Verlag, Berlin, Germany.
- Touma and Vauclin, 1986. Touma, J. and Vauclin, M. (1986), Experimental and numerical analysis of two-phase infiltration in a partially saturated soil. *Transport Porous Med.*, 1, 26-55.
- Vauclin et al., 1979. Vauclin, M., Khanji, D., and Vachaud, G. (1979), Experimental and numerical study of a transient, two-dimensional unsaturated-saturated water table recharge problem. *Water Resources Res.*, 15(5), 1089-1101.